J. Am. Chem. Soc. **2000,** *122,* 10273−10281

Increasing the Diameter of Cylindrical and Spherical Supramolecular Dendrimers by Decreasing the Solid Angle of Their Monodendrons via Periphery Functionalization

Virgil Percec,*,† Wook-Dong Cho,† and Goran Ungar‡

Contribution from the Roy & Diana Vagelos Laboratories, Department of Chemistry, University of Pennsylvania, Philadelphia, Pennsylvania 19104-6323, and Department of Engineering Materials and Center for Molecular Materials, University of Sheffield, Sheffield S1 3JD, U.K.

Received July 6, 2000

Abstract: The synthesis of three generations of self-assembling monodendrons based on an internal AB_3 3,4,5-trisubstituted benzyl ether repeat unit containing an AB_2 3,4-bis[*p*-(*n*-dodecan-1-yloxy)benzyloxy]benzyl ether monodendron **[(*4-3,4*)12G1-X]** attached on the periphery and the structural analysis of the corresponding supramolecular dendrimers by X-ray diffraction (XRD) experiments are described. The results from these experiments are compared with data reported previously from our laboratory on three generations of monodendrons based on the same internal AB_3 repeat unit containing an AB_3 3,4,5-tris[*p*-(*n*-dodecan-1-yloxy)-benzyloxy]benzyl ether monodendron **[(*4-3,4,5*)12G1-X]** on the periphery (Percec, V.; Cho, W.-D.; Mosier, P. E.; Ungar, G.; Yeardley, D. J. P. *J. Am. Chem. Soc.* **1998,** *120*, 11061). In both series of monodendrons, the solid angle of the monodendron increases with the increase of the generation number. As a result, the increase in the diameter of the cylindrical and spherical supramolecular dendrimers is smaller than the one expected from the fully extended monodendritic repeat unit. For the same internal repeat unit, the solid angle of the monodendron is determined by the solid angle of the unit attached to its periphery. The **(*4-3,4*)12G1-X** AB_2 group attached to the periphery of the monodendrons decreases their solid angle by comparison with the series containing the **(*4-3,4,5*)12G1-X** AB_3 group on their periphery, and subsequently, the AB_2 group increases the diameter of the supramolecular dendrimers. The elucidation of this architectural effect clarifies some of the current limitations and provides new strategies for the design of functional nanosystems from dendritic building blocks.

Introduction

In a series of publications from our laboratory, we have reported the elaboration of synthetic and structural analysis strategies that are currently employed in the design of monodendritic building blocks that self-assemble in bulk into spherical,[1−4] cylindrical,[2,3,5,6] and more complex[7] supramolecular and macromolecular dendrimers. The spherical supramolecular and macromolecular dendrimers self-organize in $Pm\bar{3}n$[1a,2] and $Im\bar{3}m$[4] cubic lattices, while the cylindrical supramolecular and macromolecular dendrimers self-organize in a *p*6*mm*[5] hexagonal columnar lattice (Scheme 1). The reversible and irreversible interconversion of these lattices and of their supramolecular dendrimers is also of interest to researchers in our laboratory (Scheme 1).[1b,d,3] These lattices provided access to the determination of the shape and size of supramolecular dendrimers and of the corresponding monodendrons by X-ray diffraction experiments.[1a,4,5,7] Since both self-organizing[8] and non-self-

---

* To whom correspondence should be addressed. E-mail: percec@sas.upenn.edu.

† University of Pennsylvania.

‡ University of Sheffield.

(1) (a) Balagurusamy, V. S. K.; Ungar, G.; Percec, V.; Johansson, G. *J. Am. Chem. Soc.* **1997**, *119*, 1539. (b) Percec, V.; Cho, W.-D.; Mosier, P. E.; Ungar, G.; Yeardley, D. J. P. *J. Am. Chem. Soc.* **1998**, *120*, 11061. (c) Percec, V.; Cho, W.-D.; Möller, M.; Prokhorova, S. A.; Ungar, G.; Yeardley, D. J. P. *J. Am. Chem. Soc.* **2000**, *122*, 4249. (d) Ungar, G.; Percec, V.; Holerca, M. N.; Johansson, G.; Heck, J. *Chem. Eur. J.* **2000**, *6*, 1258.

(2) Hudson, S. D.; Jung, H.-T.; Percec, V.; Cho, W.-D.; Johansson, G.; Ungar, G.; Balagurusamy, V. S. K. *Science* **1997**, *278*, 449.

(3) Percec, V.; Ahn, C.-H.; Ungar, G.; Yeardley, D. J. P.; Möller, M.; Sheiko, S. S. *Nature* **1998**, *391*, 161.

(4) Yeardley, D. J. P.; Ungar, G.; Percec, V.; Holerca, M. N.; Johansson, G. *J. Am. Chem. Soc.* **2000**, *122*, 1684.

(5) (a) Percec, V.; Johansson, G.; Heck, J.; Ungar, G.; Batty, S. V. *J. Chem. Soc., Perkin Trans. 1* **1993**, 1411. (b) Percec, V.; Heck, J. A.; Tomazos, D.; Ungar, G. *J. Chem. Soc., Perkin Trans. 2* **1993**, 2381. (c) Percec, V.; Heck, J.; Tomazos, D.; Falkenberg, F.; Blackwell, H.; Ungar, G. *J. Chem. Soc., Perkin Trans. 1* **1993**, 2799. (d) Percec, V.; Tomazos, D.; Heck, J.; Blackwell, H.; Ungar, G. *J. Chem. Soc., Perkin Trans. 2* **1994**, 31. (e) Johansson, G.; Percec, V.; Ungar, G.; Abramic, D. *J. Chem. Soc., Perkin Trans. 1* **1994**, 447. (f) Percec, V.; Johansson, G.; Ungar, G.; Zhou, J. *J. Am. Chem. Soc.* **1996**, *118*, 9855. (g) Percec, V.; Cho, W.-D.; Ungar, G.; Yeardley, D. J. P. *Angew. Chem.* **2000**, *112*, 1661; *Angew. Chem., Int. Ed.* **2000**, *39*, 1597.

(6) (a) Percec, V.; Schlueter, D.; Ungar, G.; Cheng, S. Z. D.; Zhang, A. *Macromolecules* **1998**, *31*, 1745. (b) Percec, V.; Ahn, C.-H.; Cho, W.-D.; Jamieson, A. M.; Kim, J.; Leman, T.; Schmidt, M.; Gerle, M.; Möller, M.; Prokhorova, S. A.; Sheiko, S. S.; Cheng, S. Z. D.; Zhang, A.; Ungar, G.; Yeardley, D. J. P. *J. Am. Chem. Soc.* **1998**, *120*, 8619. (c) Prokhorova, S. A.; Sheiko, S. S.; Möller, M.; Ahn, C.-H.; Percec, V. *Macromol. Rapid Commun.* **1998**, *19*, 359. (d) Percec, V.; Schlueter, D. *Macromolecules* **1997**, *30*, 5783. (e) Kwon, Y. K.; Chvalun, S. N.; Blackwell, J.; Percec, V.; Heck, J. A. *Macromolecules* **1995**, *28*, 1552. (f) Chvalun, S. N.; Blackwell, J.; Cho, J. D.; Bykova, I. V.; Percec, V. *Acta Polym.* **1999**, *50*, 51. (g) Kwon, Y. K.; Chvalun, S. N.; Schneider, A.-I.; Blackwell, J.; Percec, V.; Heck, J. A. *Macromolecules* **1994**, *27*, 6129. (h) Percec, V.; Schlueter, D.; Kwon, Y. K.; Blackwell, J.; Möller, M.; Slangen, P. *Macromolecules* **1994**, *28*, 8807. (i) Johansson, G.; Percec, V.; Ungar, G.; Zhou, J. P. *Macromolecules* **1996**, *29*, 646. (j) Percec, V.; Johansson, G.; Schlueter, D.; Ronda, J. C.; Ungar, G. *Macromol. Symp.* **1996**, *101*, 43. (k) Percec, V.; Ahn, C.-H.; Cho, W.-D.; Johansson, G.; Schlueter, D. *Macromol. Symp.* **1997**, *118*, 33.

(7) (a) Percec, V.; Chu, P.; Ungar, G.; Zhou, J. *J. Am. Chem. Soc.* **1995**, *117*, 11441. (b) Percec, V.; Ahn, C.-H.; Bera, T. K.; Ungar, G.; Yeardley, D. J. P. *Chem. Eur. J.* **1999**, *5*, 1070.

10.1021/ja0024643 CCC: $19.00

Scheme 1. Schematic Representation of (A) the Self-Assembly of Building Blocks Based on Flat Tapered Monodendrons into Supramolecular Cylindrical Dendrimers and Their Subsequent Self-Organization in a *p*6*mm* Hexagonal Columnar (Φ_h) Lattice and (B) the Self-Assembly of the Conical and Hemispherical Monodendrons into Supramolecular Spherical Dendrimers and Their Subsequent Self-Organization in $Pm\bar{3}n$ and $Im\bar{3}m$ Cubic (Cub) Lattices

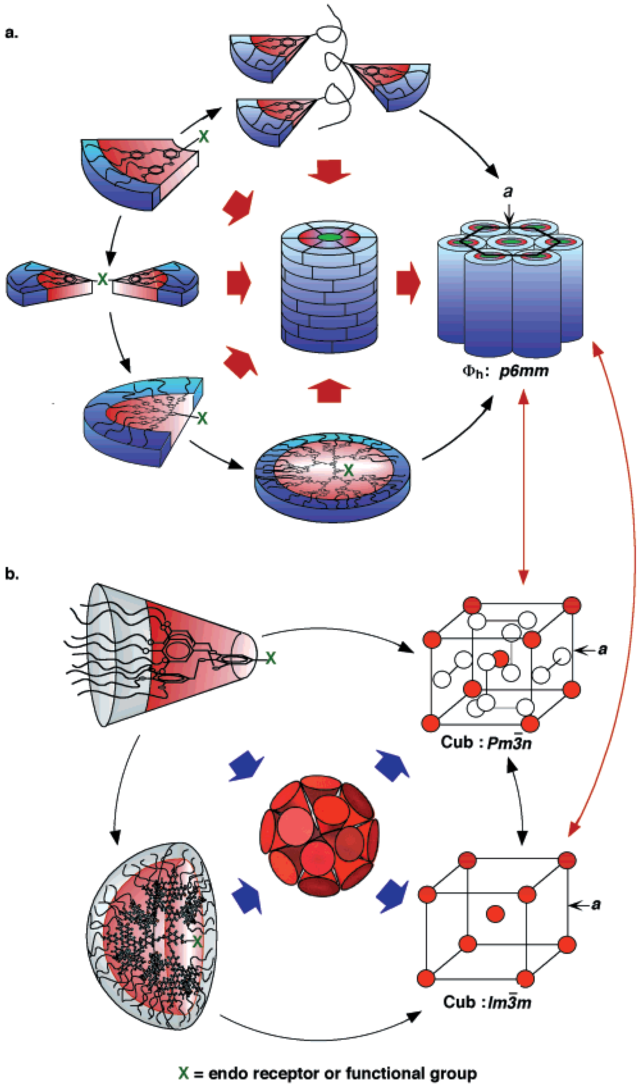

organizing[9] building blocks derived from dendritic units are used for the construction of functional nanosystems, the elucidation of the structural principles involved in their self-assembly and self-organization are of general interest.

Most of the monodendritic building blocks investigated in our laboratory are based on an AB_3 3,4,5-trisubstituted benzyl ether repeat unit.[1−7] Three libraries containing from three to five generations of AB_3 benzyl ether monodendrons[1a−c] with different first-generation monodendritic units on their periphery were investigated to establish the structural parameters that govern the shape and size of the higher generation monodendrons and of the corresponding supramolecular dendrimers in bulk state. The structure and shape of the second-generation monodendrons and supramolecular dendrimers from these three libraries together with their structural parameters obtained from the X-ray analysis of their lattices are summarized in Scheme 2. As observed from this scheme, for the same internal repeat unit, the shape and size of monodendrons and supramolecular dendrimers are determined mainly by the structure of the monodendritic unit attached to their periphery and, to less extent, by the functional group from their apex. For example, the replacement of a 3,4,5-tris(*n*-dodecan-1-yloxy)benzyl ether[1a] from the periphery of **(*3,4,5*)^{2}12G2-X** with a 3,4,-bis(*n*-dodecan-1-yloxy)benzyl ether[1c] group provides **(*3,4-3,4,5*)12G2-X** (Scheme 2). This structural change increases both the diameter of the supramolecular spherical dendrimer from $D = 42.4$ Å to $D = 51.8$ Å and the number of conical monodendrons required to assemble the spherical dendrimer from $\mu = 12$ to $\mu = 28$. Simultaneously, the replacement of the 3,4,5-tris(*n*-dodecan-1-yloxy)benzyl ether[1a] from the periphery of **(*3,4,5*)^{2}12G2-X** with 3,4,5-tris[*p*-(*n*-dodecan-1-yloxy)benzyloxy]benzyl ether[1b] produces **(*4*-(*3,4,5*)^2)12G2-X** (Scheme 2). This architectural modification changes the shape of the supramolecular dendrimer from spherical to cylindrical.

A recent publication from our laboratory[1d] demonstrated that the size and shape of a supramolecular dendrimer are determined by the solid angle of the monodendron. In that publication, it was shown that the solid angle of a monodendron is determined by the volume of the functionality present in the monodendron apex.[1d] Therefore, the solid angle of the monodendron seems to be determined both by the volume of the functionality from the dendritic apex and by the architecture of the repeat unit from its periphery. Consequently, we have decided to investigate the capability of the monodendritic unit from the periphery toward the control of the solid angle of the monodendron in order to correlate the effect of its architecture with the size and shape of the resulting supramolecular dendrimer. This publication describes the synthesis and the structural analysis of the first three generations of AB_3 3,4,5-trisubstituted benzyl ether monodendrons containing on their periphery a 3,4-bis[*p*-(*n*-dodecan-1-yloxy)benzyloxy]benzyl ether AB_2 group **[(*4-3,4*)-12G1-X]**. This is the fourth and the last library from the series of self-assembling AB_3 monodendrons.[1a−c] This library is complementary to the one containing the 3,4,5-tris[*p*-(*n*-dodecan-1-yloxy)benzyloxy]benzyl ether AB_3 group **[(*4-3,4,5*)12G1-X]** on the periphery (see the last column in Scheme 2)[1b] and will demonstrate the complexity involved in the design of supramolecular dendrimers via their periphery functionalization approach.

Results and Discussion

The synthesis of methyl 3,4-bis[*p*-(*n*-dodecan-1-yloxy)benzyloxy]benzyl ether benzoate **[(*4-3,4*)12G1-CO_2CH_3]** is outlined in Scheme 3. The detailed synthesis of this compound was reported previously.[6b] It follows the procedure elaborated in our laboratory for the synthesis of methyl 3,4,5-tris[*p*-(*n*-dodecan-1-yloxy)benzyloxy]benzoate **[(*4-3,4,5*)12G1-CO_2CH_3]**.[1b] 3,4-Bis[*p*-(*n*-dodecan-1-yloxy)benzyloxy]benzoic acid **[(*4-3,4*)-12G1-COOH]** was prepared by the basic hydrolysis of **(*4-3,4*)12G1-CO_2CH_3** as reported previously.[6b] The synthesis of the next two generations of monodendrons was performed via

---

(8) (a) Pesak, D. J.; Moore, J. S. *Angew. Chem., Int. Ed. Engl.* **1997**, *36*, 1636. (b) Suárez, M.; Lehn, J.-M.; Zimmerman, S. C.; Skoulios, A.; Heinrich. B. *J. Am. Chem. Soc.* **1998**, *120*, 9526. (c) Meier, H.; Lehmann, M. *Angew. Chem., Int. Ed.* **1998**, *37*, 643.

(9) (a) Fréchet, J. M. J. *Science* **1994**, *263*, 1710. (b) Tomalia, D. A. *Adv. Mater.* **1994**, *6*, 529. (c) Newkome, G. R.; Moorefield, C. N.; Vögtle, F. *Dendritic Molecules. Concepts, Synthesis, Perspectives*; VCH: Weinheim, 1996. (d) Moore, J. S. *Acc. Chem. Res.* **1997**, *30*, 402. (e) Zeng, F.; Zimmerman, S. C. *Chem. Rev.* **1997**, *97*, 1681. (f) Fischer, M.; Vögtle, F. *Angew. Chem., Int. Ed.* **1999**, *38*, 884. (g) Bosman, A. W.; Janssen, H. M.; Meijer, E. W. *Chem. Rev.* **1999**, *99*, 1665. (h) Moore, J. S. *Curr. Opin. Colloid Interface Sci.* **1999**, *4*, 108. (i) Schlüter, A. D.; Rabe, J. P. *Angew. Chem., Int. Ed.* **2000**, *39*, 864. (j) Jang, W.-D.; Jiang, D.-L.; Aida, T. *J. Am. Chem. Soc.* **2000**, *122*, 3232.

Scheme 2. Structural Analysis of AB_3 Trisubstituted Second-Generation Monodendrons and Supramolecular Dendrimers Containing on Their Periphery Various AB_3 or AB_2 Monodendrons[a]

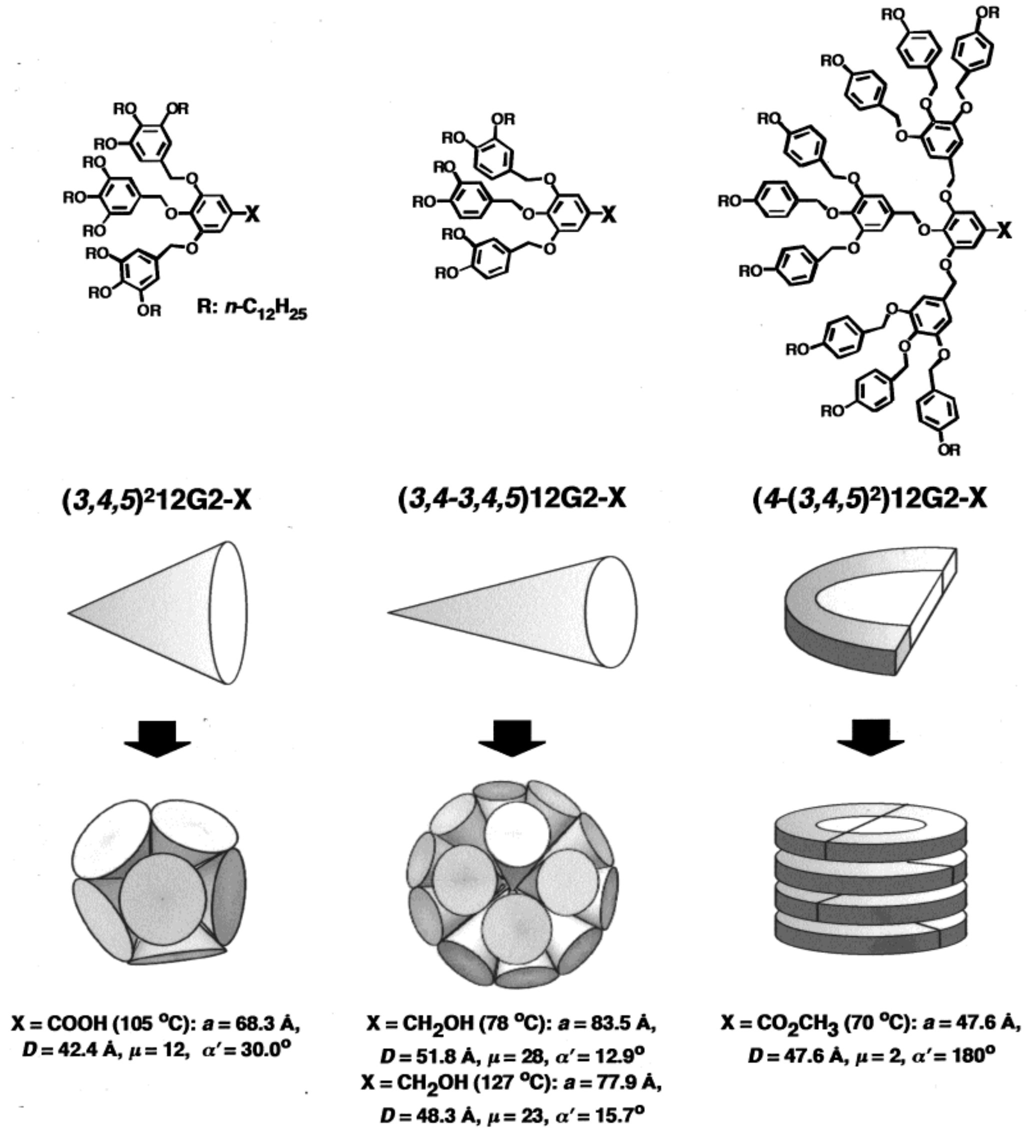

[a] Data are from refs 1a−c.

a convergent approach[10] and follows the general procedure elaborated in our laboratory for the synthesis of monodendritic benzyl ethers.[1a−c] In this particular case, it involves the reduction of **(*4-3,4*)12G1-CO_2CH_3** with $LiAlH_4$ in THF to produce **(*4-3,4*)12G1-CH_2OH** in 94.5% yield, followed by chlorination with $SOCl_2$ in CH_2Cl_2 in the presence of 2,6-di-*tert*-butyl-4-methylpyridine (**DTBMP**)[1a−c,12] proton trap to produce **(*4-3,4*)-12G1-CH_2Cl** in 100% yield. Etherification of methyl 3,4,5-trihydroxybenzoate with freshly prepared **(*4-3,4*)12G1-CH_2Cl** was performed in a mixture of THF/DMF = 200/30 at 70 °C in the presence of K_2CO_3 as base for 4 h. **(*4-3,4-3,4,5*)12G2-CO_2CH_3** was obtained in 76.3% yield after purification by column chromatography (basic Al_2O_3, CH_2Cl_2) and recrystallization from a mixture of acetone/CH_2Cl_2 (1/3, 500 mL). Reduction of **(*4-3,4-3,4,5*)12G2-CO_2CH_3** with $LiAlH_4$ in THF produced **(*4-3,4-3,4,5*)12G2-CH_2OH** in 86.7% yield. Its chlorination with $SOCl_2$ in the presence of DTBMP produced **(*4-3,4-3,4,5*)12G2-CH_2Cl**, which was used without purification in the etherification of methyl 3,4,5-trihydroxybenzoate (DMF/THF = 140/40 (v/v) in the presence of K_2CO_3 at 70 °C). After 6 h of reaction time, **(*4-3,4-*(*3,4,5*)^2)12G3-CO_2CH_3** was obtained in 46.8% yield after purification by column chromatography (basic Al_2O_3, CH_2Cl_2) and recrystallization from acetone/CH_2Cl_2 = 1/3.

The structure of monodendrons and intermediary compounds was confirmed by a combination of ^1H NMR, ^{13}C NMR, thin-layer chromatography (TLC), high-pressure liquid chromatography (HPLC), elemental analysis, and gel permeation chromatography (GPC). The quantitative etherification of the methyl 3,4,5-trihydroxybenzoate was monitored by the disappearance of the benzylic CH_2Cl protons at 4.50 ppm in the ^1H NMR spectrum and of the **(*4-3,4-*(*3,4,5*)$^{n-1}$)12G*n*-CH_2Cl** peak in HPLC. Figure 1 shows representative GPC traces of **(*4-3,4*)-12G1-CO_2CH_3, (*4-3,4-3,4,5*)12G2-CO_2CH_3,** and **(*4-3,4-*(*3,4,5*)^2)-12G3-CO_2CH_3** monodendrons. The 2-fold increase in molecular weight from generation one to generation two and the 3-fold increase from generation two to generation three allows the monitoring of the etherification process by both HPLC and GPC since all GPC traces are well separated (Figure 1). The difference between the theoretical and experimental molecular weights (relative to polystyrene standards) is due to the difference

---

(10) Hawker, C.; Fréchet, J. M. J. *J. Am. Chem. Soc.* **1990**, *112*, 7638.

(11) Ungar, G.; Abramic, D.; Percec, V.; Heck, J. A. *Liq. Cryst.* **1996**, *21*, 73.

Scheme 3. Synthesis of ***(4-3,4-(3,4,5)$^{n-1}$)12Gn-X*** (X = CO_2CH_3, CH_2OH, and CH_2Cl) Monodendrons[a]

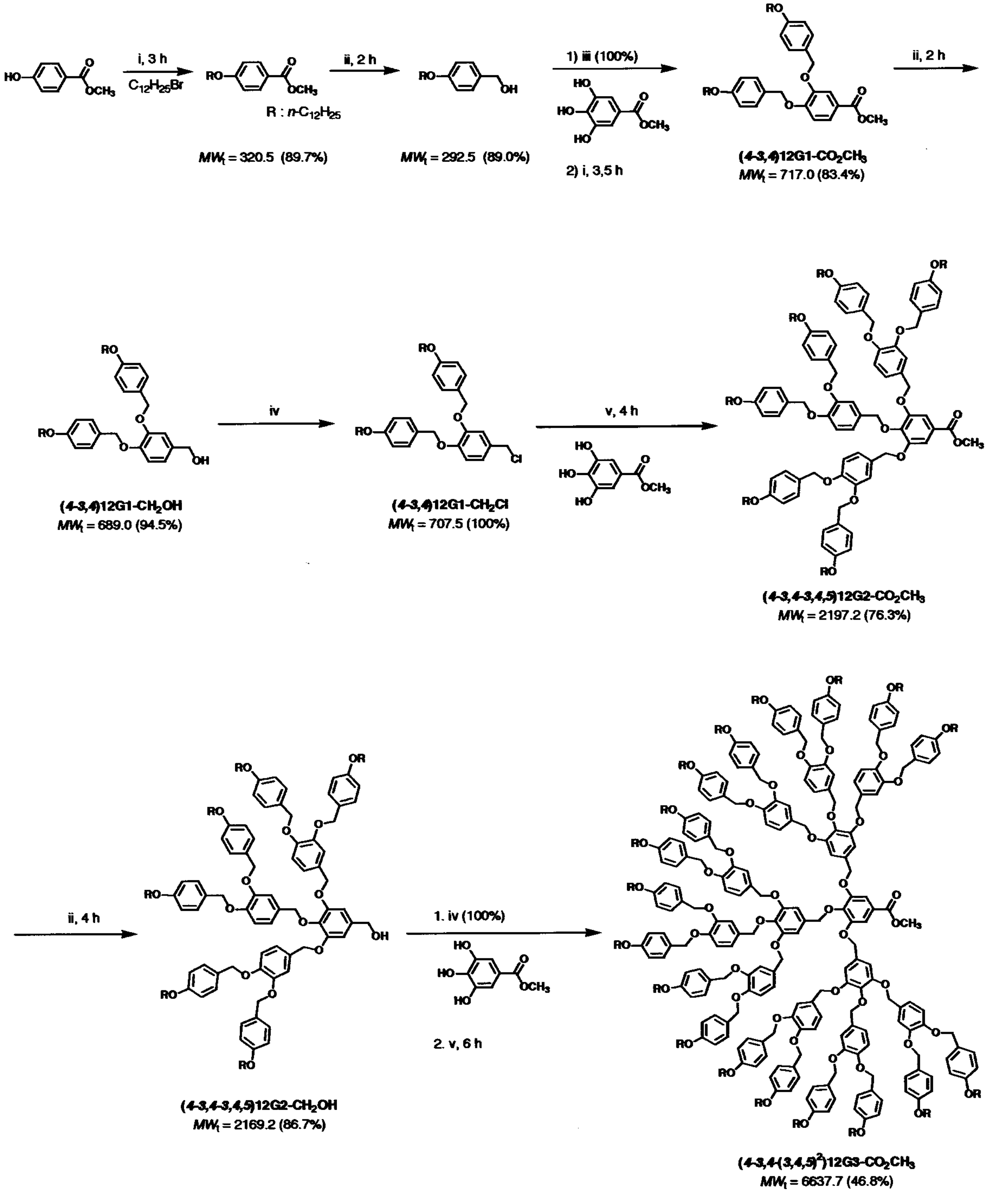

[a] Reagents and conditions: (i) K_2CO_3, DMF, 70 °C; (ii) $LiAlH_4$, THF, 20 °C; (iii) $SOCl_2$, CH_2Cl_2, DMF (catalytic), 20 °C; (iv) $SOCl_2$, DTBMP, CH_2Cl_2, 20 °C; (v) K_2CO_3, DMF, THF, 70 °C.

between the hydrodynamic volume of polystyrene and of the monodendrons and agrees with previous results for our laboratory.[1a]

The structural analysis of the supramolecular dendrimers self-assembled in bulk from these monodendrons was carried out by a combination of differential scanning calorimetry (DSC), thermal optical polarized microscopy (TOPM), and X-ray diffraction (XRD) experiments according to standard methods used in our laboratory.[1,4-7] The transition temperatures together with the corresponding enthalpy changes are summarized in Table 1. ***(4-3,4)*12G1-CO$_2$CH$_3$** displays a monotropic hexagonal columnar (Φ_h) phase. ***(4-3,4)*12G1-COOH** exhibits an enantiotropic Φ_h phase. ***(4-3,4-3,4,5)*12G2-CO$_2$CH$_3$** and ***(4-3,4-(3,4,5)^2)*12G3-CO$_2$CH$_3$** display enantiotropic cubic (Cub) phases. All supramolecular dendrimers display additional crystalline phases which were not analyzed in detail by XRD. The d-spacings of the Φ_h and Cub lattices are reported in Table 2. The results from Table 2 were used to assign the lattice symmetries[1a,d,5f] and subsequently to calculate, with the aid of densities (ρ_{20}), the data from Table 3. Table 3 summarizes the lattice symmetry, lattice dimensions (a) of all supramolecular dendrimers, their experimental diameter (D_{exp}), the diameter of the supramolecular dendrimer based on the fully extended conformation of two monodendrons (D_{ext}), the number of mono-

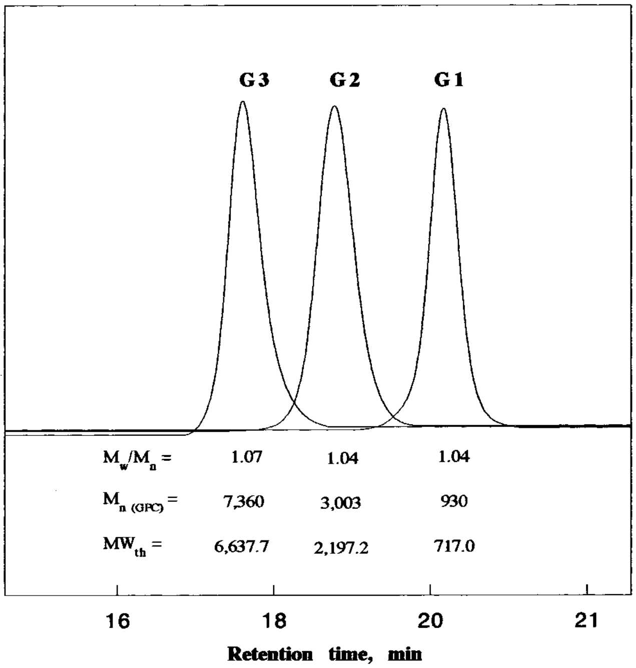

Figure 1. GPC traces with M_n and M_w/M_n values determined by GPC with polystyrene standards for **(*4-3,4-*(*3,4,5*)$^{n-1}$)12G*n*-CO$_2$CH$_3$** with $n = 1-3$.

dendrons that form a $Pm\bar{3}n$ lattice (μ') and a spherical supramolecular dendrimer (μ), the number of monodendrons that form a 4.7 Å cross section[11] of the cylindrical supramolecular dendrimer or a spherical supramolecular dendrimer (μ), the projection of the solid angle (i.e., the planar angle) of the tapered and conical monodendrons (α′ in °), and the density at 20 °C (ρ_{20}). The structural analysis results from Table 3 were used to generate the schematic of self-assembly outlined in the upper part of Scheme 4. As illustrated by this scheme, **(*4-3,4*)-12G1-X** displays a tapered shape while **(*4-3,4-3,4,5*)12G2-X** and **(*4-3,4-*(*3,4,5*)^2)12G3-X** exhibit conical shapes. Twelve **(*4-3,4*)12G1-CO$_2$CH$_3$**, and respectively eleven **(*4-3,4*)12G1-COOH**, tapered monodendrons self-assemble in a 4.7 Å cross section of a cylindrical supramolecular dendrimer which self-organizes in a *p*6*mm* hexagonal columnar lattice. Forty-three **(*4-3,4-3,4,5*)12G2-CO$_2$CH$_3$**, and respectively thirteen **(*4-3,4-*(*3,4,5*)^2)12G3-CO$_2$CH$_3$**, conical monodendrons self-assemble in spherical supramolecular dendrimers that self-organize in a $Pm\bar{3}n$ cubic lattice.

The solid angle of the conical monodendron is defined as $\alpha = 4\pi/\mu$, where μ is the number of monodendrons that self-assemble in a spherical supramolecular dendrimer. The projection of the solid angle of the conical monodendron provides the planar angle defined as $\alpha' = \alpha/2 = 2\pi/\mu$. The projection of the solid angle of the tapered monodendron gives a planar angle that is also $\alpha' = 2\pi/\mu$. Therefore, the solid angle of a

Table 1. Theoretical and Experimental (by GPC) Molecular Weights and Thermal Transitions of Selected Examples **(*4-3,4-*(*3,4,5*)$^{n-1}$)12G*n*-X** (***n*** = 1−3) Monodendrons

		M_n	M_w/M_n	thermal transitions (°C) and corresponding enthalpy changes (kcal/mol)[a]	
monodendron	MW$_{th}$	(GPC)	(GPC)	heating	cooling
(*4-3,4*)12G1-CO$_2$CH$_3$	717.0	930	1.04	k[b] 4 (1.96) k 60 (12.57) k 90 (0.11) k 99 (4.87) i[c] k 7 (1.64) k 55 (3.22) Φ_h[d] 60 (2.03) i	i 54 (1.92) Φ_h 2 (2.51) k −24 (0.04) k
(*4-3,4*)12G1-COOH	703.0	967	1.05	k −9 (9.89) Φ_h 125 (18.17) i k −9 (1.19) Φ_h 125 (19.22) i	i 114 (1.00) Φ_h 110 (15.37) Φ_h −15 (0.75) k
(*4-3,4-3,4,5*)12G2-CO$_2$CH$_3$	2197.2	3003	1.04	k −13 (8.61) k 74 (1.53) Cub[e] 183 (11.83) i k −21 (7.55) k 70 (0.95) Cub 182 (10.58) i	i 178 (10.37) Cub 43 (1.54) k −20 (4.52) k
(*4-3,4-*(*3,4,5*)^2)12G3-CO$_2$CH$_3$	6637.7	7360	1.07	k −16 (22.91) Cub 228 i[f,g]	

[a] Data from the first heating and cooling scans are on the first line and data from the second heating are on the second line. [b] k = crystalline. [c] i = isotropic temperature. [d] Φ_h = hexagonal columnar *p*6*mm* lattice. [e] Cub = cubic $Pm\bar{3}n$ lattice. [f] Observed by thermal optical polarized microscopy. [g] Decomposition after first heating scan.

Table 2. Measured *d*-Spacings of the Hexagonal Columnar and Cubic Lattices of Selected Examples of **(*4,3,4-*(*3,4,5*)$^{n-1}$)12G*n*-X** (***n*** = 1−3) Monodendrons

monodendron	*T* (°C)	100 (Å)	110 (Å)	200 (Å)	210 (Å)	211 (Å)	220 (Å)	310 (Å)	222 (Å)	320 (Å)	321 (Å)	400 (Å)	420 (Å)	421 (Å)	332 (Å)	422 (Å)
(*4-3,4*)12G1-CO$_2$CH$_3$	57	49.7	28.9	24.9												
(*4-3,4*)12G1-COOH	77	46.6														
(*4-3,4-3,4,5*)12G2-CO$_2$CH$_3$	117			53.2	47.6	43.5	37.9	33.8	31.0	29.7	28.6	26.8	23.9	23.3	21.9	21.5
(*4-3,4-*(*3,4,5*)^2)12G3-CO$_2$CH$_3$	177		73.4	51.9	46.5	42.5	36.8	32.9	30.1	28.9	27.9	26.1	23.3	22.8		

Table 3. Structural Analysis of Supramolecular Dendrimers Self-Assembled from Selected Examples of **(*4,3,4-*(*3,4,5*)$^{n-1}$)12G*n*-X** (***n*** = 1−3) Monodendrons

monodendron	*T* (°C)	lattice	$\langle d_{100}\rangle$[a] (Å)	*a* (Å)	D_{exp} (Å)	D_{ext}[f] (Å)	μ'	μ	α′[j]	ρ_{20}[k] (g/cm^3)
(*4-3,4*)12G1-CO$_2$CH$_3$	57	*p*6*mm*	49.9	57.6[b]	57.6[d]	58.7		12[k]	30.0	1.05
(*4-3,4*)12G1-COOH	77	*p*6*mm*	46.6	53.8[b]	53.8[d]	56.1		11[h]	32.7	1.04
(*4-3,4-3,4,5*)12G2-CO$_2$CH$_3$	117	$Pm\bar{3}n$		106.5[c]	66.1[e]	70.7	344[g]	43[i]	8.4	1.04
(*4-3,4-*(*3,4,5*)^2)12G3-CO$_2$CH$_3$	177	$Pm\bar{3}n$		104.1[c]	64.6[e]	82.7	105[g]	13[i]	27.7	1.03

[a] $\langle d_{100}\rangle = (d_{100} + \sqrt{3}d_{110} + 2d_{200})/3$. [b] Hexagonal columnar lattice parameter $a = 2\langle d_{100}\rangle/\sqrt{3}$. [c] Cubic lattice parameter $a = (\sqrt{2}d_{110} + \sqrt{4}d_{200} + \sqrt{5}d_{210} + \sqrt{6}d_{211} + \sqrt{8}d_{220} + \sqrt{10}d_{310} + \sqrt{12}d_{222} + \sqrt{13}d_{320} + \sqrt{14}d_{321} + \sqrt{16}d_{400} + \sqrt{20}d_{420} + \sqrt{21}d_{421} + \sqrt{22}d_{332} + \sqrt{24}d_{422})/14$. [d] Columnar diameter $D_{exp} = 2\langle d_{100}\rangle/\sqrt{3}$. [e] Spherical diameter $D_{exp} = 2\sqrt[3]{3a^3/32\pi}$. [f] D_{ext} = diameter of fully extended cylindrical or spherical dendrimers. [g] Number of monodendrons per unit cell $\mu' = (a^3N_A\rho)/M$. [h] Number of monodendrons per cylinder stratum of the supramolecular cylinder $\mu = (\sqrt{3}N_AD^2_{exp}t\rho)/2M$ (Avogadro's number, $N_A = 6.022045 \times 10^{23}$ mol^{-1}; the average height of the column stratum $t = 4.7$ Å; M = molecular mass of monodendron) (for details, see ref 5a). [i] Number of monodendrons per spherical dendrimer $\mu = \mu'/8$. [j] Projection of the solid angle for tapered and conical monodendron $\alpha' = 360/\mu$ (deg). [k] ρ_{20} = experimental density at 20 °C.

Scheme 4. Structural Analysis of Three Generations of ***(4-3,4-(3,4,5)***$^{n-1}$**)12G*n*-X** and ***(4-(3,4,5)***^{n}**)12G*n*-X** Monodendrons and of Their Supramolecular Dendrimers[a]

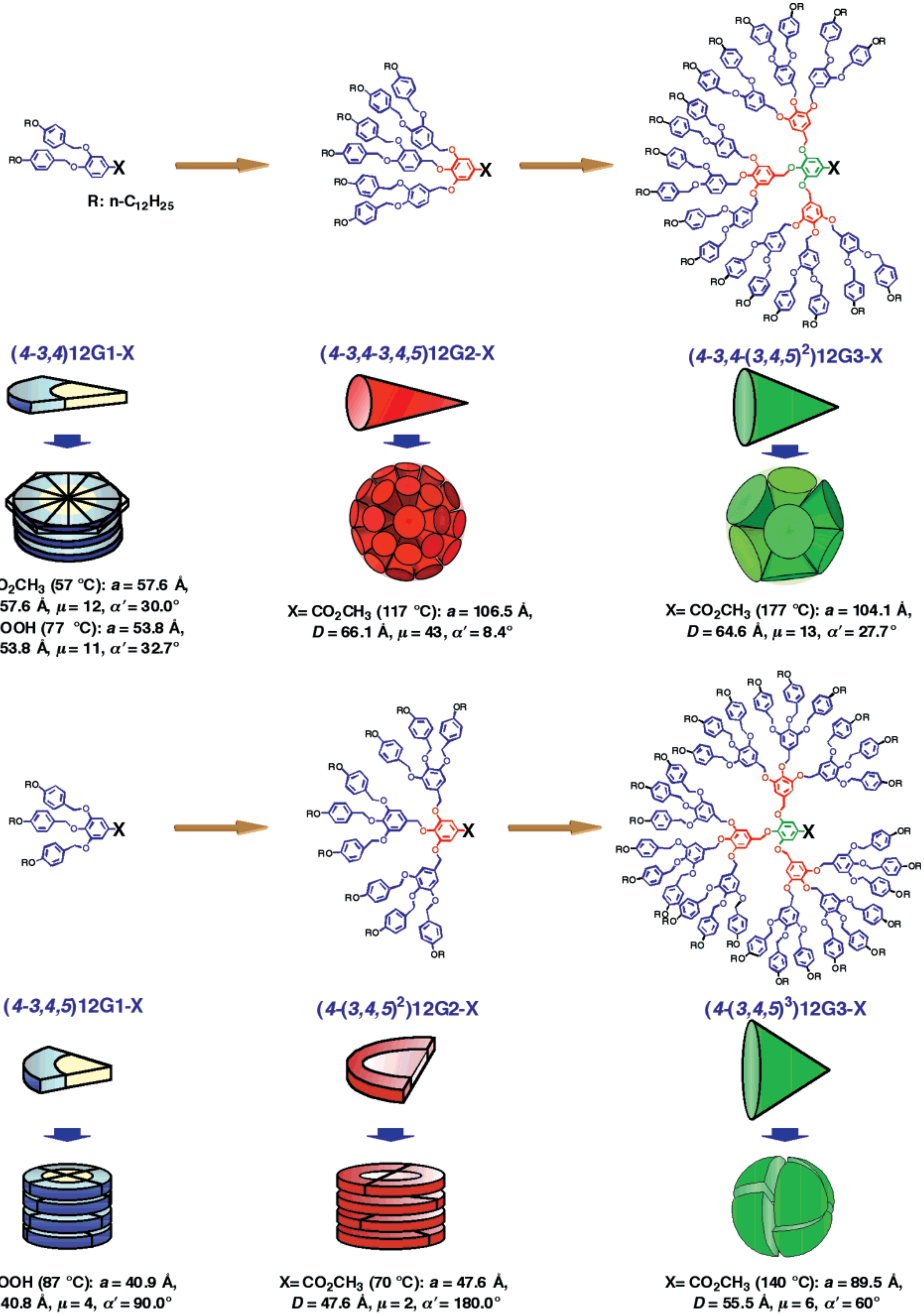

---

[a] Data for and **(*4-*(*3,4,5*)^{n})12G*n*-X** are from ref 1b. *a* (Å), lattice dimension; *D* (Å), diameter of the supramolecular columnar or spherical dendrimer; μ, number of monodendrons forming a 4.7 Å cross section of the supramolecular cylindrical dendrimer or the number of monodendrons forming the spherical supramolecular dendrimer; α′ (deg), projection of the solid angle for tapered and conical monodendrons. The temperature of the XRD experiment in (°C) is reported between parentheses.

Scheme 5. Hierarchical Development of a Single-Sphere Monodendron Starting from Tapered or Conical Monodendrons

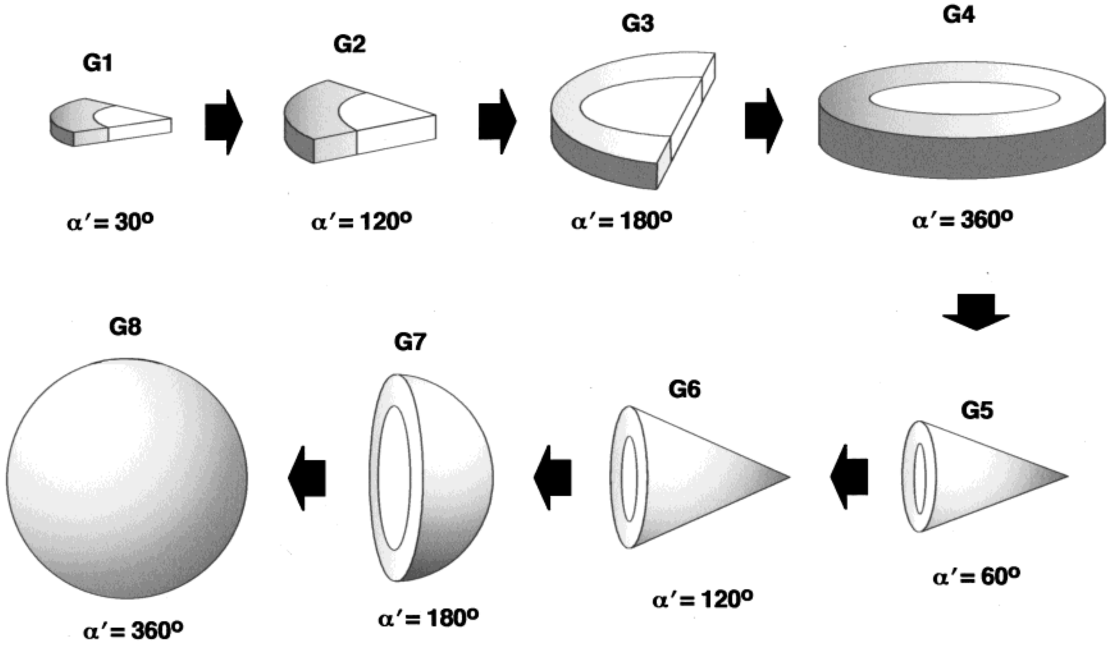

monodendron is directly proportional to its projected planar angle. Table 3 lists the values of the projections of the solid angle (α'), since they can be visualized for both the cases of tapered and conical monodendrons much more easily than their corresponding solid angles. The comparison of the D_{exp}, μ, and α' for **(*4-3,4-3,4,5*)12G2-X** and for **(*4-3,4-*(*3,4,5*)^2)12G3-X** (Table 3 and Scheme 4) provides the most significant result. Although the transition from generation two to generation three should increase the theoretical radius of the fully extended supramolecular dendrimer with one benzyl ether unit (i.e., 6.0 Å) and the corresponding diameter with two benzyl ether units (i.e., 12.0 Å), the experimental diameter of the third generation, at the temperature at which it was determined, is lower than that of the second generation supramolecular dendrimer (64.6 Å vs 66.1 Å). This is partially due to the increase in α' from 8.4° to 27.7° and partially due to the higher temperature of the XRD experiment (177 °C for G3 versus 117 °C for G2). It is well established that the diameter of the supramolecular spherical dendrimers decreases with the increase in temperature.[1d] The second column from Scheme 2 provides an example which shows that a 49 °C increase in temperature decreases the diameter by 3.5 Å. Although this comparison has only a relative meaning, correcting for the difference in temperature cannot bring the diameter to the expected value. Therefore, in contrast to the expected trend, when the generation number is increased, the diameter of the spherical supramolecular dendrimer increases much less than expected from its theoretical fully extended length of the aromatic part i.e., 12.0 Å per generation.

To compare the contribution of the solid or planar angle of the monodendron as it is determined by the structure of the repeat unit from its periphery, we compare in Scheme 4 the influence of μ and α' on D_{exp} of supramolecular dendrimers generated by the two libraries of monodendrons that have on their periphery 3,4,5-tris[*p*-(*n*-dodecan-1-yloxy)benzyloxy]benzyl ether[1b] AB_3 groups (lower part of Scheme 4) and respectively 3,4-bis[*p*-(*n*-dodecan-1-yloxy)benzyloxy]benzyl ether AB_2 groups (upper part of Scheme 4). This comparison can be made only at the same generation number, where the theoretical diameter of the fully extended monodendron is identical regardless of the nature of the two different monodendritic units on their periphery. Scheme 4 is almost self-explanatory. **(*4-3,4,5*)12G1-X** self-assembles in a supramolecular cylinder that has a diameter that is between 13 and 17 Å smaller than the one generated from **(*4-3,4*)12G1-X**. The difference between these two dissimilar D_{exp} values that have identical fully extended theoretical diameters is determined by the number of monodendrons required to form the cross section of the supramolecular cylinder and their corresponding solid angle, i.e., $\mu = 4$ ($\alpha' = 90°$) for the case of **(*4-3,4,5*)12G1-X** and respectively $\mu = 11$ ($\alpha' = 32.7°$) or 12 ($\alpha' = 30.0°$) for the case of **(*4-3,4*)12G1-X.** The number of monodendrons required to create a supramolecular dendrimer is proportional to the planar angle α', i.e., $\mu = 4$ provides $\alpha' = 90°$, while $\mu = 12$ and respectively 11 provide $\alpha' = 30.0°$ and respectively 32.7°. Therefore, a larger μ provides a smaller α' and a larger diameter. The attachment of AB_3 and AB_2 monodendrons to the periphery of the AB_3 monodendrons transplants this trend from the first generation to the second and respectively to the third-generation monodendrons as well as to their corresponding supramolecular dendrimers (Scheme 4). At the second generation the two supramolecular dendrimers have different shapes i.e., cylindrical and spherical, and therefore, a direct comparison cannot be made. However, at the third generation the diameters of the two spherical supramolecular dendrimers follow the same trend as that of the corresponding first-generation cylindrical supramolecular dendrimers, i.e., the **(*4-3,4-*(*3,4,5*)^2)12G3-X**-derived supramolecular dendrimer has a diameter that is larger than that of the **(*4-*(*3,4,5*)^3)12G3-X**-derived supramolecular dendrimer with 9.1 Å. This is in spite of the fact that the former was determined at 177 °C and the latter at 140 °C. At the same temperature this difference would have to be even larger since with increasing the temperature the diameter decreases.[1d] This result is complementary to that obtained with **(*4-3,4*)12G1-X** and **(*4-3,4,5*)-12G1-X** and demonstrates the capability to increase the diameter of both cylindrical and spherical supramolecular dendrimers based on the same internal repeat unit by attaching monodendrons of lower solid angle on their periphery. However, regardless of the repeat unit on their periphery and, therefore, of the initial solid angle of the monodendron, upon increasing the generation number the tapered monodendron changes its shape by becoming a half of a disk,[1b] a disklike molecule,[5g] and subsequently adopts a conical shape[5g] (Scheme 5). A conical monodendron[1a] becomes hemispherical and ultimately a single sphere.[1c] This trend is illustrated in Scheme 5. The maximum size of the cylindrical and spherical supramolecular dendrimers constructed via these principles is therefore limited.

Conclusions

The results described in this publication demonstrate a very clear trend. With increasing generation number, the solid angle of the conical and flat tapered monodendrons increases, and as a consequence the diameter of the resulting supramolecular dendrimer increases with a much lower value than the one expected from its fully extended conformation. For the same generation number constructed from AB_3 internal repeat units, the solid angle of the monodendron and the diameter of the supramolecular dendrimer are determined by the solid angle of the monodendritic repeat unit attached to the periphery. An AB_2 vs AB_3 repeat unit on the periphery decreases the overall solid angle of the monodendron and subsequently increases the diameter of the corresponding supramolecular dendrimer. These results suggest an upper limit of the size of the supramolecular dendrimers that can be constructed via the current synthetic methodology. Upon increasing the generation number, all monodendrons increase their solid angle until they become a single sphere.[1c] Therefore, the control of the size of supramolecular dendrimers synthesized from a certain repeat unit is determined both by the solid angle of the repeat unit attached to their periphery as demonstrated in this publication and by the volume of the functionality in their apex.[1d] These two architectural parameters determine the solid angle of the self-assembling monodendron and can be used to control the diameter of the supramolecular dendrimer up to the generation number before the monodendron shape becomes spherical. These results show some of the limitations of the dendritic architectural motifs but also open numerous new strategies for the design of functional nanosystems.

Experimental Section

A. Materials. Methyl 4-hydroxybenzoate (99%), 1-bromododecane (97%), 3,4-dihydroxybenzoic acid (97%), methyl 3,4,5-trihydroxybenzoate (98%), $LiAlH_4$ (95+%), $SOCl_2$ (99.5+%) (all from Aldrich), anhydrous K_2CO_3, DMF, and acetone (from Fisher, ACS. reagent) were all used as received. THF (from Fisher, ACS reagent) was refluxed over sodium ketyl until the solution turned purple and then distilled before use. CH_2Cl_2 (from Fisher, ACS. reagent) was dried over CaH_2 and freshly distilled before use.

B. Techniques. ^1H NMR (200 MHz) and ^{13}C NMR (50 MHz) spectra were recorded on a Varian Gemini 200 spectrometer at 20 °C with tetramethylsilane (TMS) as internal standard. The purity of products was determined by a combination of thin-layer chromatography (TLC) on silica gel plates (Kodak) with fluorescent indicator and high-pressure liquid chromatography (HPLC) using a Perkin-Elmer Series 10 high-pressure liquid chromatograph equipped with an LC-100 column oven, a Nelson Analytical 900 series integrator data station, and two Perkin-Elmer PL gel columns of 5×10^2 and 1×10^4 Å. THF was used as solvent at an oven temperature of 40 °C. Detection was by UV absorbance at 254 nm. Relative weight-average (M_w) and number-average (M_n) molecular weights were determined on the same instrument from a calibration plot constructed with polystyrene standards. Thermal transitions were measured on a Perkin-Elmer DSC-7 differential scanning calorimer (DSC) equipped with a TADS data station. In all cases, the heating and cooling rates were 10 °C/min. First-order transition temperatures were reported as the maxima and minima of their endothermic and exothermic peaks. Indium and zinc were used as calibration standards. An Olympus BX-40 thermal optical polarized microscope (TOPM) (100× magnification) equipped with a Mettler FP 82 hot stage and a Mettler FP 80 central processor was used to verify thermal transitions and characterize the anisotropic textures. Small-angle X-ray diffractograms (SAXD) from powder samples were recorded with a quadrant detector at Station 8.2 of the Synchrotron Radiation Source at Daresbury, UK. Small- and wide-angle X-ray diffractograms from monodomain samples were recorded with an image plate area detector (MAR Research) using graphite-monochromatized Cu Kα radiation. In both cases, samples in glass capillaries were held in a custom-built temperature cell controlled to within ±0.1 °C. The beampath up to the beamstop was either evacuated or flushed with N_2. Densities (ρ_{20}) were determined by flotation in gradient columns at 20 °C. Elemental analyses of all new compounds (M-H-W Laboratories, Phoenix, AZ) agree with the calculated value within ±0.4%.

C. Synthesis. 2,6-Di-*tert*-butyl-4-methylpyridine (**DTBMP**),[12] methyl *p*-(*n*-dodecan-1-yloxy)benzoate,[13] *p*-(*n*-dodecan-1-yloxy)benzyl alcohol,[14] *p*-(*n*-dodecan-1-yloxy)benzyl chloride,[6b] methyl 3,4-bis[*p*-(*n*-dodecan-1-yloxy)benzyloxy]benzoate **[(*4-3,4*)12G1-CO_2CH_3]**,[6b] and 3,4-bis[*p*-(*n*-dodecan-1-yloxy)benzyloxy]benzoic acid **[(*4-3,4*)12G1-COOH]**[6b] were synthesized as described previously.

General Procedure for the Synthesis of (*4-3,4-*(*3,4,5*)$^{n-1}$)12G*n*-CH_2OH. 3,4-Bis[*p*-(*n*-dodecan-1-yloxy)benzyloxy]benzyl Alcohol [(*4-3,4*)12G1-CH_2OH]. The benzyl alcohol was synthesized by the reduction of the methyl 3,4-bis[*p*-(*n*-dodecan-1-yloxy)benzyloxy]benzoate **[(*4-3,4*)12G1-CO_2CH_3]** with $LiAlH_4$. Into a three-neck round-bottom flask, equipped with a condenser, an ice bath, an N_2 inlet−outlet, and a Teflon-coated magnetic stirrer, containing a suspension of $LiAlH_4$ (8.26 g, 0.218 mol) in dry THF (900 mL), was added **(*4-3,4*)12G1-CO_2CH_3** (130 g, 0.181 mol) slowly under a flow of N_2, and the mixture was stirred for 2 h at room temperature. The reduction was shown to be complete by TLC and ^1H NMR analyses. The reaction mixture was quenched by successive dropwise addition of 9 mL of H_2O, 9 mL of 15% NaOH, and 27 mL of H_2O. At this point, H_2 evolution ceased. The granular salts were filtered and washed with THF. The solvent was distilled on a rotary evaporator, and the remaining solid was recrystallized from acetone/CH_2Cl_2 (5:1, 1000 mL) to yield 118 g (94.5%) of white crystals. Purity (HPLC): 99+%. Isotropic temperature: 97 °C. TLC (3/1 hexane/EtOAc): $R_f = 0.25$. ^1H NMR ($CDCl_3$, δ, ppm, TMS): 0.89 (t, 6H, CH_3, $J = 6.6$ Hz), 1.28 (m, 36H, $CH_3(CH_2)_9$), 1.79 (m, 4H, CH_2CH$_2$OAr), 3.96 (t, 4H, CH$_2$CH_2OAr, $J = 6.5$ Hz), 4.58 (s, 2H, CH_2OH), 5.07 (s, 2H, ArCH_2OAr, 4 position), 5.08 (s, 2H, ArCH_2OAr, 3 position), 6.84−6.94 (overlapped m, 6H, Ar*H* meta to CH_2OAr, 3,4 positions, Ar*H* (5) meta to CH_2OH, Ar*H* (6) ortho to CH_2OH), 7.00 (d, 1H, Ar*H* (2) ortho to CH_2OH, $J = 1.7$ Hz), 7.30−7.37 (overlapped m, 4H, Ar*H* ortho to CH_2OAr, 3,4 positions). ^{13}C NMR ($CDCl_3$, δ, ppm, TMS): 14.1 (CH_3), 22.7 (CH_2-CH_3), 26.0 ($CH_2CH_2CH_2OAr$), 29.3 ($CH_3(CH_2)_2CH_2$), 29.6 ($CH_3(CH_2)_3$-$(CH_2)_5$), 30.4 (CH_2CH_2OAr), 31.9 ($CH_3CH_2CH_2$), 64.9 (CH_2OH), 67.9 (CH_2CH_2OAr, 3,4-(4′) positions), 71.0 (ArCH_2OAr, 3 position), 71.3 (ArCH_2OAr, 4 position), 114.2 (Ar*C* (5) meta to CH_2OH), 114.3 (Ar*C* meta to CH_2OAr, 3,4 positions), 115.4 (Ar*C* (2) ortho to CH_2OH), 120.0 (Ar*C* (6) ortho to CH_2OH), 129.0 (Ar*C* ipso to CH_2OAr, 3,4 positions, Ar*C* ortho to CH_2OAr, 3,4 positions), 134.5 (Ar*C* ipso to CH_2OH), 149.2 (Ar*C* (3) meta to CH_2OH, Ar*C* para to CH_2OH), 158.8 (Ar*C* para to CH_2OAr, 3,4 positions). Anal. Calcd for $C_{45}H_{68}O_5$: C, 78.44; H, 9.95. Found: C, 78.33; H, 9.97.

General Procedure for the Synthesis of Benzyl Chlorides. Benzyl chlorides were synthesized by the chlorination of the corresponding benzyl alcohols with $SOCl_2$ in the presence of DTBMP.

3,4-Bis[*p*-(*n*-dodecan-1-yloxy)benzyloxy]benzyl Chloride [(*4-3,4*)-12G1-CH_2Cl]. Into a 250-mL one-neck round-bottom flask, equipped with a magnetic stirrer and an addition funnel, were placed **(*4-3,4*)-12G1-CH_2OH** (5.00 g, 7.26 mmol) and DTBMP (2.98 g, 14.5 mmol) in dry CH_2Cl_2 (100 mL). A mixture of $SOCl_2$ (0.864 g, 7.26 mmol) and CH_2Cl_2 (10 mL) was added dropwise at room temperature. After the addition was complete, quantitative conversion was observed by a combination of ^1H NMR spectroscopy and TLC. The solvent was

---

(12) Anderson, A. G.; Stang, P. J. *J. Org. Chem.* **1976**, *41*, 3034.

(13) Metzger, R. M.; Wiser, D. C.; Laidlaw, R. K.; Takassi, M. A.; Mattern, D. L.; Panetta, C. A. *Langmuir* **1990**, *6*, 350.

(14) Percec, V.; Heck, J. *J. Polym. Sci., Part A: Polym. Chem.* **1991**, *29*, 591.

distilled on a rotary evaporator, and the product was used immediately in the next step.

General Procedure for the Synthesis of (*4-3,4-*(*3,4,5*)$^{n-1}$)12G*n*-CO$_2$CH$_3$. Methyl 3,4,5-Tris{3′,4′-bis[*p*-(*n*-dodecan-1-yloxy)benzyloxy]benzyloxy}benzoate [(*4-3,4-3,4,5*)12G2-CO$_2$CH$_3$]. (*4-3,4-3,4,5*)12G2-CO$_2$CH$_3$ was synthesized according to a procedure elaborated in our laboratory.[1,4−7] In a three-neck round-bottom flask equipped with a condenser, an N$_2$ inlet−outlet, and a Teflon-coated magnetic stirrer, a mixture of K$_2$CO$_3$, DMF, and THF was thoroughly bubbled with N$_2$ for 1 h to eliminate O$_2$. Methyl 3,4,5-trihydroxybenzoate was added, and the mixture was heated to 70 °C, and then **(*4-3,4*)12G1-CH$_2$Cl** was added. After 3−5 h, the reaction was shown to be complete by a combination of TLC and ^{1}H NMR analyses. Starting from 1.79 g (9.72 mmol) of methyl 3,4,5-trihydroxybenzoate, 20.6 g (29.1 mmol) of **(*4-3,4*)12G1-CH$_2$Cl**, and 12.1 g (87.6 mmol) of K$_2$CO$_3$ in a mixture of 200 mL of DMF and 20 mL of THF at 70 °C after 4 h, 16.3 g (76.3%) of white crystals was obtained after purification by column chromatography (basic, Al$_2$O$_3$; CH$_2$Cl$_2$) and recrystallization from acetone/CH$_2$Cl$_2$ (3:1, 500 mL). Purity (HPLC): 99+%. TLC (3/1 hexane/EtOAc): $R_f = 0$. ^{1}H NMR (CDCl$_3$, δ, ppm, TMS): 0.88 (t, 18H, C*H*$_3$, $J = 6.9$ Hz), 1.26 (m, 108H, CH$_3$(C*H*$_2$)$_9$), 1.76 (m, 12H, C*H*$_2$CH$_2$OAr), 3.84−3.96 (overlapped m, 15H, CH$_2$C*H*$_2$OAr, CO$_2$C*H*$_3$), 4.75 (s, 2H, ArC*H*$_2$OAr, 4-(3′) position), 4.90 (s, 2H, ArC*H*$_2$OAr, 4-(4′) position), 4.97 (s, 8H, ArC*H*$_2$OAr, 3,5-(3′,4′) positions), 5.01 (s, 6H, ArC*H*$_2$OAr, 3,4,5 positions), 6.75−6.90 (overlapped m, 18H, Ar*H* meta to CH$_2$OAr, 3,4,5-(3′,4′) positions, Ar*H* (5′) meta to CH$_2$OAr, 3,4,5 positions, Ar*H* (6′) ortho to CH$_2$OAr, 3,4,5 positions), 7.06 (d, 3H, Ar*H* (2′) ortho to CH$_2$OAr, 3,4,5 positions, $J = 2.9$ Hz), 7.19−7.31 (overlapped m, 12H, Ar*H* ortho to CH$_2$OAr, 3,4,5-(3′,4′) positions), 7.37 (s, 2H, Ar*H* ortho to CO$_2$CH$_3$). ^{13}C NMR (CDCl$_3$, δ, ppm, TMS): 14.2 (*C*H$_3$), 22.7 (*C*H$_2$CH$_3$), 26.1 (*C*H$_2$CH$_2$CH$_2$OAr), 29.4 (CH$_3$(CH$_2$)$_2$*C*H$_2$), 29.7 (CH$_3$(CH$_2$)$_3$(*C*H$_2$)$_5$), 30.5 (*C*H$_2$CH$_2$OAr), 32.0 (CH$_3$CH$_2$*C*H$_2$), 52.2 (CO$_2$*C*H$_3$), 67.6−68.0 (CH$_2$*C*H$_2$OAr, 3,4,5-[3′,4′-(4″)] positions), 70.5−71.2 (Ar*C*H$_2$OAr, 3,4,5-(3′,4′) positions and 3,5 positions), 74.8 (Ar*C*H$_2$OAr, 4 position), 109.4 (Ar*C* ortho to CO$_2$CH$_3$), 113.9−115.1 (Ar*C* meta to CH$_2$OAr, 3,4,5-(3′,4′) positions, Ar*C* (2′) ortho to CH$_2$OAr, 3,4,5 positions, Ar*C* (5′) meta to CH$_2$OAr, 3,4,5 positions), 120.8 (Ar*C* (6′) ortho to CH$_2$OAr, 3,5 positions), 121.6 (Ar*C* (6′) ortho to CH$_2$OAr, 4 position), 125.4 (Ar*C* ipso to CO$_2$CH$_3$), 128.7−129.0 (Ar*C* ipso to CH$_2$OAr, 3,4,5-(3′,4′) positions, Ar*C* ortho to CH$_2$OAr, 3,4,5-(3′,4′) positions), 129.9 (Ar*C* ipso to CH$_2$OAr, 3,4,5 positions), 142.2 (Ar*C* para to CO$_2$CH$_3$), 148.9 (Ar*C* para to CH$_2$OAr, 3,4,5 positions), 149.3 (Ar*C* (3′) meta to CH$_2$OAr, 3,4,5 positions), 152.6 (Ar*C* meta CO$_2$CH$_3$), 158.9 (Ar*C* para to CH$_2$OAr, 3,4,5-(3′,4′) positions), 166.3 (*C*O$_2$CH$_3$). Anal. Calcd for C$_{143}$H$_{206}$O$_{17}$: C, 78.17; H, 9.45. Found: C, 78.13; H, 9.57.

3,4,5-Tris{3′,4′-bis[*p*-(*n*-dodecan-1-yloxy)benzyloxy]benzyloxy}benzyl Alcohol [(*4-3,4-3,4,5*)12G2-CH$_2$OH]. Starting from **(*4-3,4-3,4,5*)12G2-CO$_2$CH$_3$** (4.5 g, 2.05 mmol) and LiAlH$_4$ (0.09, 0.002 mol) in THF (140 mL) (4 h reaction time), a white solid (3.85 g, 86.7%) was obtained after recrystallization from a mixture of acetone/CH$_2$Cl$_2$ (1:2, 200 mL). Purity (HPLC): 99+%. Isotropic temperature: 197 °C. TLC (9/1 CH$_2$Cl$_2$/hexane): $R_f = 0.18$. ^{1}H NMR (CDCl$_3$, δ, ppm, TMS): 0.88 (t, 18H, C*H*$_3$, $J = 6.8$ Hz), 1.26 (m, 108H, CH$_3$(C*H*$_2$)$_9$), 1.74 (m, 12H, C*H*$_2$CH$_2$OAr), 3.84−3.96 (overlapped m, 12H, CH$_2$C*H*$_2$OAr), 4.54 (s, 2H, C*H*$_2$OH), 4.77 (s, 2H, ArC*H*$_2$OAr, 4-(3′) position), 4.91 (s, 2H, ArC*H*$_2$OAr, 4-(4′) position), 4.93 (s, 2H, ArC*H*$_2$OAr, 4 position), 4.96−4.97 (overlapped s, 12H, ArC*H*$_2$OAr, 3,5-(3′,4′) positions, ArC*H*$_2$OAr, 3,5 positions), 6.62 (s, 2H, Ar*H* ortho to CH$_2$OH), 6.75−6.89 (overlapped m, 18H, Ar*H* meta to CH$_2$OAr, 3,4,5-(3′,4′) positions, Ar*H* (5′) meta to CH$_2$OAr, 3,4,5 positions, Ar*H* (6′) ortho to CH$_2$OAr, 3,4,5 positions), 7.06 (d, 3H, Ar*H* (2′) ortho to CH$_2$OAr, 3,4,5 positions, $J = 7.0$ Hz), 7.20−7.33 (overlapped m, 12H, Ar*H* ortho to CH$_2$OAr, 3,4,5-(3′,4′) positions). ^{13}C NMR (CDCl$_3$, δ, ppm, TMS): 14.1 (*C*H$_3$), 22.7 (*C*H$_2$CH$_3$), 26.1 (*C*H$_2$CH$_2$CH$_2$OAr), 29.4 (CH$_3$(CH$_2$)$_2$*C*H$_2$), 29.7 (CH$_3$(CH$_2$)$_3$(*C*H$_2$)$_5$), 30.5 (*C*H$_2$CH$_2$OAr), 31.9 (CH$_3$CH$_2$*C*H$_2$), 65.2 (*C*H$_2$OH), 68.0 (CH$_2$*C*H$_2$OAr, 3,4,5-[3′,4′-(4″)] positions), 71.2 (Ar*C*H$_2$OAr, 3,4,5-(3′,4′) positions and 3,5 positions), 74.9 (Ar*C*H$_2$OAr, 4 position), 106.6 (Ar*C* ortho to CH$_2$OH), 114.4−115.0 (Ar*C* meta to CH$_2$OAr, 3,4,5-(3′,4′) positions, Ar*C* (5′) meta to CH$_2$OAr, 3,4,5 positions), 115.1 (Ar*C* (2′) ortho to CH$_2$OAr, 3,4,5 positions), 120.4 (Ar*C* (6′) ortho to CH$_2$OAr, 3,5 positions), 121.6 (Ar*C* (6′) ortho to CH$_2$OAr, 4 position), 129.0 (Ar*C* ipso to CH$_2$OAr, 3,4,5-(3′,4′) positions, Ar*C* ortho to CH$_2$OAr, 3,4,5-(3′,4′) positions), 130.4 (Ar*C* ipso to CH$_2$OAr, 3,5 positions), 131.3 (Ar*C* ipso to CH$_2$OAr, 4 position, Ar*C* para to CH$_2$OH), 136.8 (Ar*C* ipso to CH$_2$OH), 148.8 (Ar*C* para to CH$_2$OAr, 3,4,5 positions), 149.2 (Ar*C* (3′) meta to CH$_2$OAr, 3,4,5 positions), 153.0 (Ar*C* meta CH$_2$OH), 158.8 (Ar*C* para to CH$_2$OAr, 3,4,5-(3′,4′) positions). Anal. Calcd for C$_{142}$H$_{206}$O$_{16}$: C, 78.63; H, 9.57. Found: C, 78.82; H, 9.41.

3,4,5-Tris{3′,4′-bis[*p*-(*n*-dodecan-1-yloxy)benzyloxy]benzyloxy}benzyl Chloride [(*4-3,4-3,4,5*)12G2-CH$_2$Cl]. (*4-3,4-3,4,5*)12G2-CH$_2$Cl was synthesized by the procedure described for the synthesis of **(*4-3,4*)12G1-CH$_2$Cl.** To a solution of 1.0 g (0.46 mmol) of **(*4-3,4-3,4,5*)12G2-CH$_2$OH** and 0.38 g (1.85 mmol) DTBMP in 20 mL of dry CH$_2$Cl$_2$ was added 0.055 g (0.46 mmol) of SOCl$_2$ in 20 mL of CH$_2$Cl$_2$. **(*4-3,4-3,4,5*)12G2-CH$_2$Cl** was used without purification in the next step.

Methyl 3,4,5-Tris(3′,4′,5′-tris{3″,4″-bis[*p*-(*n*-dodecan-1-yloxy)benzyloxy]benzyloxy}benzyloxy)benzoate [(*4-3,4-*(*3,4,5*)^2)12G3-CO$_2$CH$_3$]. To a solution of methyl 3,4,5-trihydroxybenzoate (0.099 g, 0.54 mmol) and K$_2$CO$_3$ (0.669 g, 4.84 mmol) in a mixture of DMF (140 mL) and THF (40 mL) was added **(*4-3,4-3,4,5*)12G2-CH$_2$Cl** (3.53 g, 1.61 mmol) at 70 °C. After 6 h the mixture was worked up as described for **(*4-3,4-3,4,5*)12G2-CO$_2$CH$_3$** to yield a white solid (1.67 g, 46.8%). Purity (HPLC): 99+%. TLC (20/1 hexane/EtOAc): $R_f = 1.00$. ^{1}H NMR (CDCl$_3$, δ, ppm, TMS): 0.89 (t, 54H, C*H*$_3$, $J = 6.6$ Hz), 1.27 (m, 324H, CH$_3$(C*H*$_2$)$_9$), 1.73 (m, 36H, C*H*$_2$CH$_2$OAr), 3.70−3.92 (overlapped m, 39H, CH$_2$C*H*$_2$OAr, CO$_2$C*H*$_3$), 4.57−5.13 (ovelapped m, 60H, ArC*H*$_2$OAr), 6.56−6.90 (overlapped m, 60H, Ar*H* meta to CH$_2$OAr, 3,4,5-[3′,4′,5′-(3″,4″)] positions, Ar*H* (5″) meta to CH$_2$OAr, 3,4,5-(3′,4′,5′) positions, Ar*H* (6″) ortho to CH$_2$OAr, 3,4,5-(3′,4′,5′) positions, Ar*H* ortho to CH$_2$OAr, 3,4,5 positions), 6.96−7.26 (overlapped m, 45H, Ar*H* ortho to CH$_2$OAr, 3,4,5-[3′,4′,5′-(3″,4″)] positions, Ar*H* (2″) ortho to CH$_2$OAr, 3,4,5-(3′,4′,5′) positions), 7.47 (s, 2H, Ar*H* ortho to CO$_2$CH$_3$). ^{13}C NMR (CDCl$_3$, δ, ppm, TMS): 14.1 (*C*H$_3$), 22.7 (*C*H$_2$CH$_3$), 26.1 (*C*H$_2$CH$_2$CH$_2$OAr), 29.3 (CH$_3$(CH$_2$)$_2$*C*H$_2$), 29.6 (CH$_3$(CH$_2$)$_3$(*C*H$_2$)$_5$), 30.5 (*C*H$_2$CH$_2$OAr), 31.9 (CH$_3$CH$_2$*C*H$_2$), 52.2 (CO$_2$*C*H$_3$), 67.4−67.8 (CH$_2$*C*H$_2$OAr, 3,4,5-{3′,4′,5′-[3″,4″-(4‴)]} positions), 71.4 (Ar*C*H$_2$OAr, 3,4,5-[3′,4′,5′-(3″,4″)] positions, 3,4,5-(3′,5′) positions and 3,5 positions), 74.8−74.9 (Ar*C*H$_2$OAr, 3,4,5-(4′) positions, 4 position), 107.0 (Ar*C* ortho CH$_2$OAr, 3,4,5 positions), 109.6 (Ar*C* ortho to CO$_2$CH$_3$), 113.5−114.7 (Ar*C* meta to CH$_2$OAr, 3,4,5-[3′,4′,5′-(3″,4″)] positions, Ar*C* (2″) ortho to CH$_2$OAr, 3,4,5-(3′,4′,5′) positions, Ar*C* (5″) meta to CH$_2$OAr, 3,4,5-(3′,4′,5′) positions), 120.6 (Ar*C* (6″) ortho to CH$_2$OAr, 3,4,5-(3′,5′) positions), 121.4 (Ar*C* (6″) ortho to CH$_2$OAr, 3,4,5-(4′) positions), 125.4 (Ar*C* ipso to CO$_2$CH$_3$), 128.1−129.1 (Ar*C* ipso to CH$_2$OAr, 3,4,5-[3′,4′,5′-(3″,4″)] positions, Ar*C* ortho to CH$_2$OAr, 3,4,5-[3′,4′,5′-(3″,4″)] positions), 130.0 (Ar*C* ipso to CH$_2$OAr, 3,4,5-(3′,4′,5′) positions), 131.1 (Ar*C* para to CH$_2$OAr, 3,5 positions), 132.2 (Ar*C* para to CH$_2$OAr, 4 position), 138.4 (Ar*C* ipso to CH$_2$OAr, 3,4,5 positions), 142.2 (Ar*C* para to CO$_2$CH$_3$), 148.8 (Ar*C* para to CH$_2$OAr, 3,4,5-(3′,4′,5′) positions), 149.2 (Ar*C* (3″) meta to CH$_2$OAr, 3,4,5-(3′,4′,5′) positions), 152.6 (Ar*C* meta to CO$_2$CH$_3$), 153.0 (Ar*C* meta to CH$_2$OAr, 3,4,5 positions), 158.7 (Ar*C* para to CH$_2$OAr, 3,4,5-[3′,4′,5′-(3″,4″)] positions), 166.3 (*C*O$_2$CH$_3$). Anal. Calcd for C$_{434}$H$_{620}$O$_{50}$: C, 78.53; H, 9.42. Found: C, 78.69; H, 9.31.

Acknowledgment. Financial support by the National Science Foundation (DMR-99-96288), the Engineering and Physical Science Research Council, UK, and the Synchrotron Radiation Source at Daresbury, UK, is gratefully acknowledged. We are also grateful to Professor S. Z. D. Cheng of University of Akron for density measurements.

JA0024643